

# Ablation of *Wntless* in endosteal niches impairs lymphopoiesis rather than HSCs maintenance

Jingjing Cao<sup>\*1</sup>, Lingling Zhang<sup>\*1</sup>, Yong Wan<sup>1</sup>, Hanjun Li<sup>1</sup>, Rujiang Zhou<sup>1</sup>, Heyuan Ding<sup>2</sup>, Yongzhong Liu<sup>3</sup>, Zhengju Yao<sup>1</sup> and Xizhi Guo<sup>1</sup>

<sup>1</sup> Bio-X Institutes, Key Laboratory for the Genetics of Developmental and Neuropsychiatric Disorders (Ministry of Education), Shanghai Jiao Tong University, Shanghai, China

<sup>2</sup> The Fifth People's Hospital of Shanghai, Fudan University, China

<sup>3</sup> Shanghai Cancer Institute, Shanghai, China

Osteoblasts and perivascular stromal cells constitute essential niches for HSC self-renewal and maintenance in the bone marrow. Wnt signaling is important to maintain HSC integrity. However, the paracrine role of Wnt proteins in osteoblasts-supported HSC maintenance and differentiation remains unclear. Here, we investigated hematopoiesis in mice with *Wntless* (*Wls*) deficiency in osteoblasts or Nestin-positive mesenchymal progenitor cells, which presumptively block Wnt secretion in osteoblasts. We detected defective B-cell lymphopoiesis and abnormal T-cell infiltration in the bone marrow of *Wls* mutant mice. Notably, no impact on HSC frequency and repopulation in the bone marrow was observed with the loss of osteoblastic *Wls*. Our findings revealed a supportive role of Wnts in osteoblasts-regulated B-cell lymphopoiesis. They also suggest a preferential niche role of osteoblastic Wnts for lymphoid cells rather than HSCs, providing new clues for the molecular nature of distinct niches occupied by different hematopoietic cells.

**Keywords:** B cell · HSC maintenance · Osteoblast · T-cell infiltration · *Wntless*



Additional supporting information may be found in the online version of this article at the publisher's web-site

## Introduction

HSCs that periodically generate all hematopoietic lineages are mostly stored in vascular or endosteal niches in the bone marrow [1]. Vascular niches consist of sinusoidal endothelium cells [2–4] whereas endosteal niches are mainly composed of osteoblasts [5, 6]. These niche cells are important to regulate HSCs self-renewal and maintenance. Recent evidence also reveals that perivascular Nestin<sup>+</sup> mesenchymal progenitor cells form a supportive niche for HSCs [3, 7, 8]. In addition, studies from Dr. Morrison suggest that HSCs mainly reside in the perivascular niches whereas the early lymphoid progenitor cells prefer to locate at endosteal niches [9, 10].

Compelling evidence reveals that Wnt signaling is an important regulator for HSCs integrity and function. Wnt proteins, which consist of 19 members in mammals, could be transduced through canonical or noncanonical signaling pathways [11].  $\beta$ -Catenin is the key and obligatory mediator of canonical Wnt signaling. Stabilized  $\beta$ -catenin expression expands the pool of HSCs and leads to deficiency in HSCs repopulation capacity [12, 13]. Conversely, deletion of  $\beta$ -catenin or *Wnt3a* leads to defective HSCs long-term maintenance [14, 15]. Nevertheless, several lines of evidence also indicate that  $\beta$ -catenin is dispensable for HSCs maintenance [16, 17]. On the other hand, inhibition of environmental canonical Wnt signaling in osteoblasts impairs HSCs self-renewal and quiescence [18]. Collectively, canonical Wnt signaling is revealed to

Correspondence: Dr. Xizhi Guo  
e-mail: xzguo2005@sjtu.edu.cn; zjyao@sjtu.edu.cn

\*These authors contributed equally to this work.

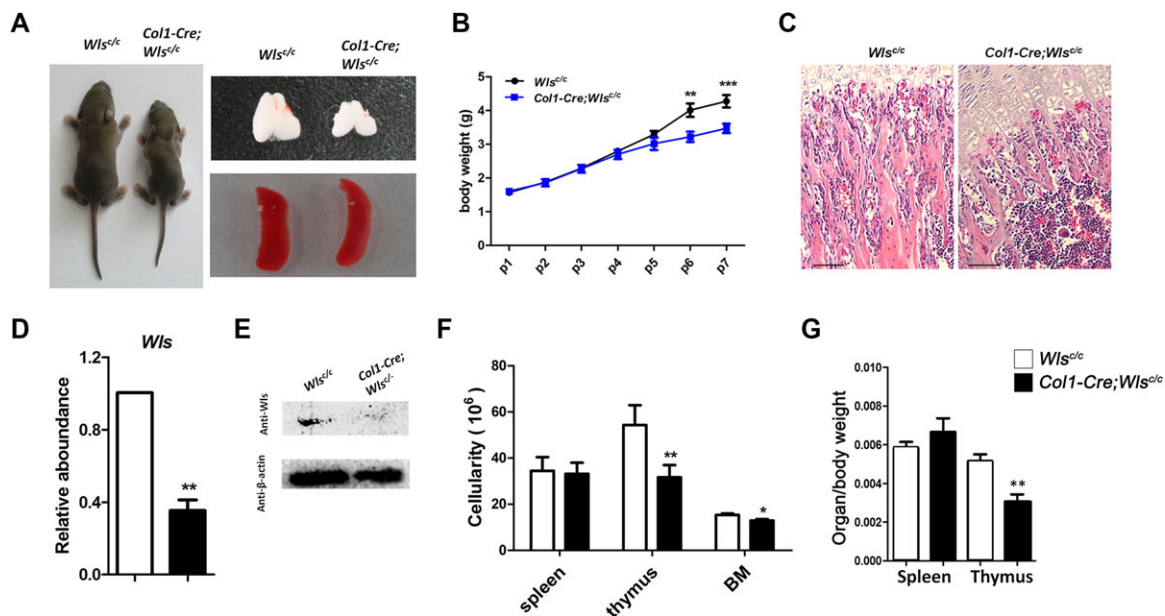


**Figure 1.** Depletion of osteoblastic *Wls* decreases the size of thymus and bone marrow. (A) Examples of whole body (left panel), thymus, and spleen size (upper right panel) of *Col1-Cre; Wls<sup>c/c</sup>* from representative mice out of seven mice analyzed are shown. (B) Growth curve of the *Col1-Cre; Wls<sup>c/c</sup>* mice compared to *Wls<sup>c/c</sup>* mice. Bars show mean  $\pm$  SEM from seven mice. \* $p < 0.05$ ; \*\* $p < 0.01$ , determined by Student's *t* test. (C) HE staining for tibia sections from the *Col1-Cre; Wls<sup>c/c</sup>* and control mice. Scale bar, 50  $\mu$ m. One representative image out of four independent experiments is shown. (D) *Wls* expression in osteoblasts was determined by qRT-PCR and normalized to  $\beta$ -actin. Expression in  $\beta$ -actin was set to 1. Bars show mean  $\pm$  SEM from three independent experiments in seven mice per group (white bar: *Wls<sup>c/c</sup>*, black bar: *Col1-Cre; Wls<sup>c/c</sup>*). \*\* $p < 0.01$ , determined by Student's *t* test. (E) *Wls* protein level in osteoblasts from *Col1-Cre; Wls<sup>c/c</sup>* mice were determined by Western blot. Beta-actin was used as loading control. One representative blot out of three independent experiments is shown. (F) The BM and thymus cellularity was determined by cell count in wild type and *Col1-Cre; Wls<sup>c/c</sup>* mutant mice. Bars show mean  $\pm$  SEM from six mice. (G) The size of thymus relative to whole body in the mutant compared to the controls. Bars show mean  $\pm$  SEM from  $n = 6$  mice. All the samples were collected at P7 for the controls and mutant mice. BM, bone marrow. \* $p < 0.05$ ; \*\* $p < 0.01$ , determined by Student's *t* test.

regulate HSCs self-renewal in a dosage-dependent manner [19]. In addition, noncanonical Wnt signaling is also reported to sustain HSCs maintenance and aging [20, 21].

Osteoblasts also support B-cell commitment and differentiation [22–24]. However, the function of Wnt signaling in osteoblast-supported B-cell development remains controversial. For instance, based on the analysis of *Lef1*, *Apc*, and *Frizzled9* knockout mutant mice, canonical Wnt signaling seems to promote the proliferation or early development of B progenitor cells [25–27]. In contrast, depletion of  $\beta$ -catenin in hematopoietic progenitor cells or mature B cells has no overt impact on B-cell development [16, 17, 28]. Moreover, overexpression of *Wnt5a* in OP9 stromal cells promotes B-cell differentiation whereas overexpression of *Wnt3a* inhibits it [29–31]. These discrepancies highlight the need of novel genetic approaches in studying the effect of Wnt signaling in osteoblast-regulated B-cell development.

*Wntless (Wls)* was first identified in the fruit fly as a GPCR cargo protein that mediates Wnt ligand secretion [32]. Inactivation of *Wls* gene blocks Wnt protein secretion in varied tissues and causes various phenotypes corresponding to Wnt signaling failure [33–37]. Deletion of *Wls* in osteoblasts impairs bone mass accrual as described in our previous report and other lab's work [38, 39]. In this study, we continued to investigate the biological activity of Wnts in endosteal niches and their effect on HSCs maintenance

and differentiation. Our results indicate important roles of Wnts in osteoblasts-supported lymphopoiesis and their relatively little influence on HSCs maintenance.

## Results

### Deletion of osteoblastic *Wls* impairs B-cell lymphopoiesis

We first investigated B-cell lymphopoiesis in *Col1-Cre; Wls<sup>c/c</sup>* mice that had osteoblast-specific *Wls* deficiency. As described previously [39], the *Col1-Cre; Wls<sup>c/c</sup>* mutant mice were of smaller size and lower bone mass (Fig. 1A). The growth curve revealed that the mutant mice displayed a significant decrease in body weight at postnatal stage P7 (Fig. 1B). Because the mutant mice only had a lifespan around two weeks, we analyzed hematopoiesis at P7, which just began to display defects in bone formation as evidenced by HE staining (Fig. 1C). qRT-PCR and Western blot analysis validated the downregulation of *Wls* in osteoblasts from mutant cortical bones at P7 (Fig. 1D and E). The relative size and cellularity of the thymus and bone marrow (BM) in the *Col1-Cre; Wls<sup>c/c</sup>* mice were significantly smaller compared to *Wls<sup>c/c</sup>* controls

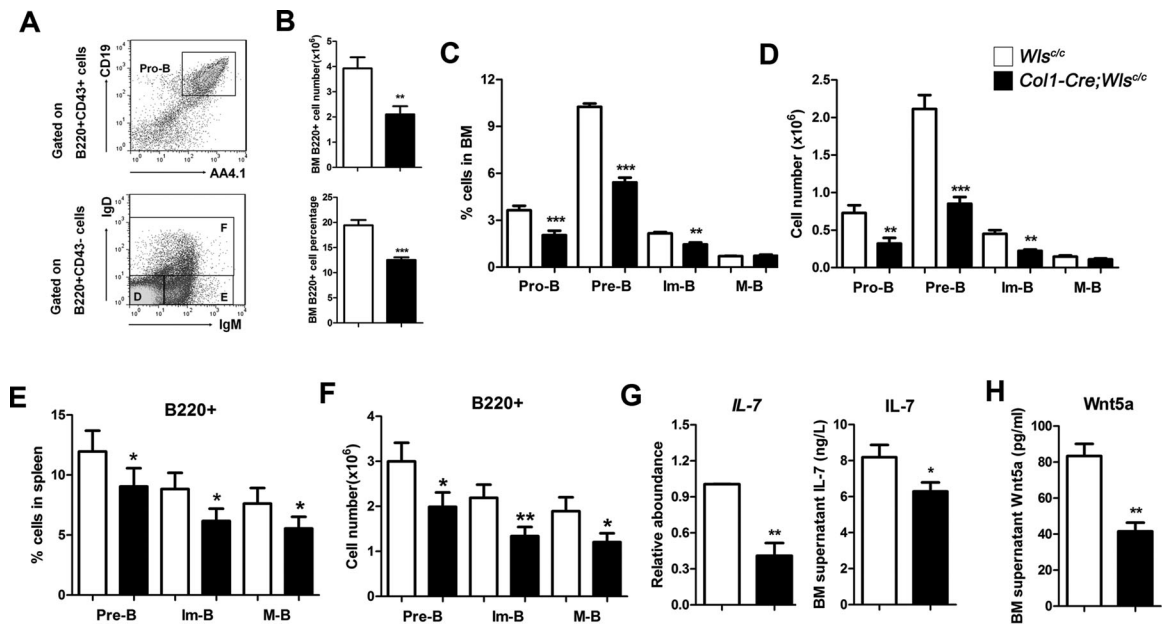


**Figure 2.** Deficiency of *Wls* in osteoblasts impairs B-cell lymphopoiesis. (A) Bone marrow cells were isolated from *Col1-Cre; Wls<sup>c/c</sup>* and analyzed for subsets of B-cell development by flow cytometry of B220, CD43, CD19, AA4.1, IgD, and IgM. One representative dot plot out of five independent experiments is shown. (B) (top) Frequencies and (bottom) absolute numbers of B220<sup>+</sup> cells in the BM of *Col1-Cre; Wls<sup>c/c</sup>* mice were determined as shown in A. Bars show means  $\pm$  SEM from  $n = 5$  mice. (C, D) (C) Frequencies and (D) absolute numbers of pro-B (B220<sup>+</sup>CD43<sup>+</sup>CD19<sup>+</sup>AA4.1<sup>+</sup>), pre-B (B220<sup>+</sup>CD43<sup>-</sup>IgD<sup>-</sup>IgM<sup>-</sup>), immature B (B220<sup>+</sup>CD43<sup>-</sup>IgM<sup>+</sup>IgD<sup>-</sup>, Im-B), and mature B (B220<sup>+</sup>CD43<sup>-</sup>IgM<sup>+</sup>IgD<sup>+</sup>, M-B) populations in BM of *Col1-Cre; Wls<sup>c/c</sup>* were determined by flow cytometry. Bars show mean  $\pm$  SEM from  $n = 5$  mice. White bar: *Wls<sup>c/c</sup>*, black bar: *Col1-Cre; Wls<sup>c/c</sup>*. (E, F) (E) Frequencies and (F) absolute numbers of pre-B (B220<sup>+</sup>CD19<sup>+</sup>), immature B (B220<sup>+</sup>IgM<sup>+</sup>, Im-B), and mature B (B220<sup>+</sup>IgD<sup>+</sup>, M-B) populations in spleen of *Col1-Cre; Wls<sup>c/c</sup>* were determined by flow cytometry. Bars show mean  $\pm$  SEM from  $n = 5$  mice. (G) (Left) Expression of *IL-7* in the osteoblasts was determined by qRT-PCR. Beta-actin was used as control and its expression was set to 1. Bars show means  $\pm$  SEM from  $n = 6$  mice representative of three independent experiments. (Right) *IL-7* protein levels in the supernatant from BM was determined by ELISA. Bars show mean  $\pm$  SEM from  $n = 6$  mice. (H) *Wnt5a* protein levels in the supernatant from BM were determined by ELISA. Bars show mean  $\pm$  SEM from  $n = 6$  mice. All the samples were collected at P7 for the controls and mutant mice. \* $p < 0.05$ ; \*\* $p < 0.01$ ; \*\*\* $p < 0.001$ , determined by Student's *t* test.

at P7 (Fig. 1A, F, and G). In contrast, the size and cellularity of the spleen were relatively normal.

Then we analyzed the subsets of B-cell population as previously described [40], which is characterized by B220<sup>+</sup>CD43<sup>+</sup>CD19<sup>+</sup>AA4.1<sup>+</sup> (pro-B cells), B220<sup>+</sup>CD43<sup>-</sup>IgD<sup>-</sup>IgM<sup>-</sup> (pre-B cells, Fraction D in Fig. 2A), B220<sup>+</sup>CD43<sup>-</sup>IgM<sup>+</sup>IgD<sup>-</sup> (immature B cell, Fraction E in Fig. 2A), and B220<sup>+</sup>CD43<sup>-</sup>IgM<sup>+</sup>IgD<sup>+</sup> (mature B cell, Fraction F in Fig. 2A), respectively. FACS analyses showed that the cellularity and percentage of total B220<sup>+</sup> B-cell lineages, pro-B, pre-B, and immature B cells were decreased in the bone marrow of *Col1-Cre; Wls<sup>c/c</sup>* mice compared to controls (Fig. 2B–D). Consistently, the size of pre-B (B220<sup>+</sup>CD19<sup>+</sup>), immature (CD19<sup>+</sup>IgM<sup>+</sup>), and mature (CD19<sup>+</sup>IgD<sup>+</sup>) B-cell pools were also smaller in the spleen of the mutants (Fig. 2E and F). In addition, ELISA examination also showed decreased *Wnt5a* protein levels in the bone marrow (Fig. 2H), indicating defects of *Wnt* secretion in *Wls*-deficient osteoblasts. Furthermore, qRT-PCR analysis detected a relative decrease of *IL-7* expression in the cortical bone of *Wls*-deficient mutant, whereas the ELISA indicated the lower *IL-7* protein level in bone marrow (Fig. 2G). The decrease of *IL-7* expression may be the secondary effect of *Wls* deficiency in osteoblasts. These findings suggest that *Wnt* proteins secreted from osteoblasts facilitate B-cell development.

### Loss of *Wls* in osteoblasts leads to T-cell infiltration in the bone marrow

T cells are differentiated from common lymphoid progenitor cells (CLP, Lin<sup>-</sup>Sca1<sup>+</sup>cKit<sup>low</sup>CD127<sup>+</sup>) in the bone marrow and become mature in the thymus. T cells migrate outwards from the thymus to peripheral blood as single CD4<sup>+</sup> or CD8<sup>+</sup> T cells and would enrich in tissues under condition of antigen-induced inflammation. We observed expanded pools of CD4<sup>+</sup> and CD8<sup>+</sup> T cells in the bone marrow of *Col1-Cre; Wls<sup>c/c</sup>* mice (Fig. 3A–C). In contrast, the frequency and cell number of CD4<sup>+</sup> and CD8<sup>+</sup> T cells was decreased in the spleen of mutant mice (Fig. 3D and E). Importantly, the majority of enriched T cells in the mutant bone marrow were CD62L<sup>+</sup> (Supporting Information Fig. 1A), indicating that they were mostly naïve and not active T cells. However, the size of naïve T-cell populations did not differ in the mutant bone marrow from the controls (Supporting Information Fig. 1B). In contrast, the frequency but not number of early T-progenitor cells (ETP, Lin<sup>-</sup>CD25<sup>-</sup>c-Kit<sup>+</sup>) was increased in the thymus of *Col1-Cre; Wls<sup>c/c</sup>* mutant mice (Fig. 3F–H). However, the frequency of CD4<sup>+</sup> or CD8<sup>+</sup> T cells was not altered in the *Col1-Cre; Wls<sup>c/c</sup>* thymus as compared to the controls (data not shown), indicating the normal frequencies of matured T cells in the mutant thymus.

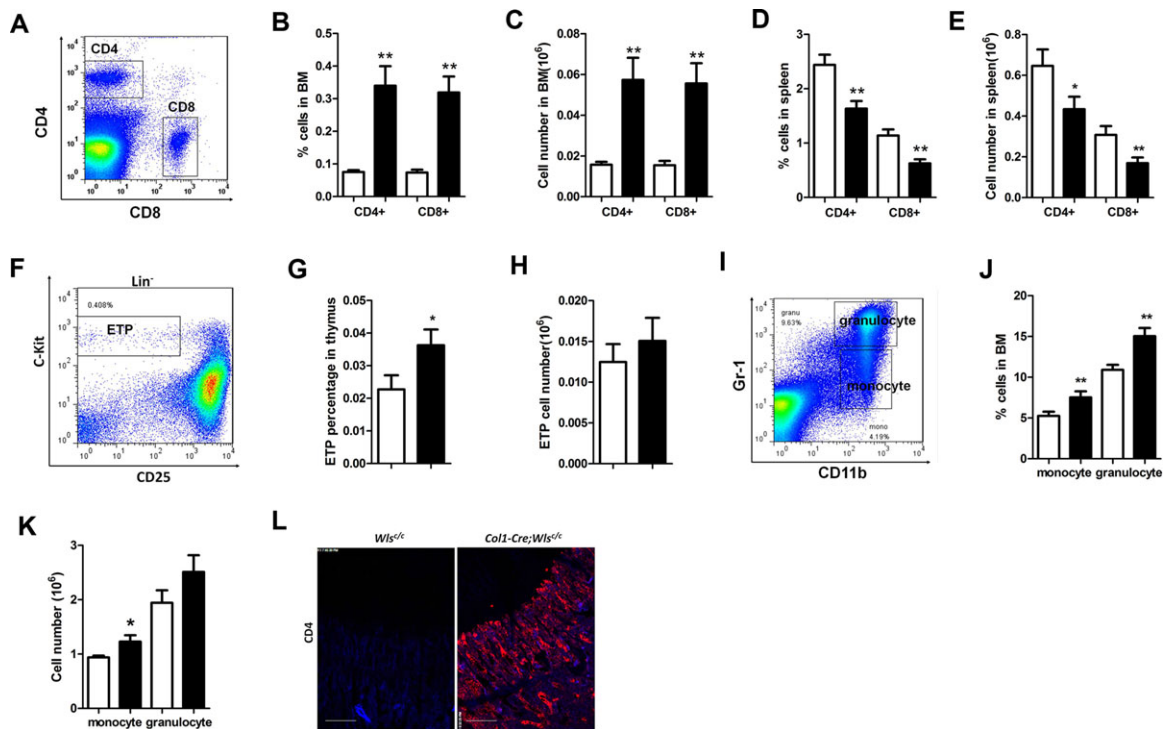


**Figure 3.** Deletion of osteoblastic *Wls* leads to naive T-cell infiltration in the bone marrow. (A) Dot plots depict the CD4<sup>+</sup> and CD8<sup>+</sup> T cells in the bone marrow. One representative dot plot out of seven independent experiments is shown. (B, C) The frequencies and number of CD4<sup>+</sup> and CD8<sup>+</sup> cells in the BM of wild type and mutant mice. Bars show means  $\pm$  SEM from  $n = 7$  mice. White bar: *Wls*<sup>c/c</sup>, black bar: *Col1-Cre; Wls*<sup>c/c</sup>. (D, E) The frequencies and number of CD4<sup>+</sup> and CD8<sup>+</sup> cells in the spleen. Bars show means  $\pm$  SEM from  $n = 7$  mice. (F) Dot plots depict the ETP cells gated by Lin<sup>-</sup>CD25<sup>-</sup>c-Kit<sup>+</sup> in the thymus. One representative dot plot out of seven independent experiments is shown. (G, H) The frequency (G), but not the cellularity (H) of ETP was increased in the thymus of *Col1-Cre; Wls*<sup>c/c</sup> mice. Bars show means  $\pm$  SEM from  $n = 7$  mice. (I) Dot plots depict the CD11b<sup>+</sup>Gr1<sup>low</sup> monocytes and CD11b<sup>+</sup>Gr1<sup>high</sup> granulocytes. One representative dot plot out of seven independent experiments is shown. (J, K) The frequencies and number of the monocytes and granulocytes in the BM. Bars show means  $\pm$  SEM from  $n = 7$  mice. (L) IHC with anti-CD4 in the sections from the BM of wild type and *Wls* mutants. Bar, 40  $\mu$ m. One representative picture out of three independent experiments is shown. All the samples were collected at P7 for the controls and mutant mice. BM, bone marrow. \* $p < 0.05$ , determined by Student's *t* test.

We also detected a relative increase in the cell number and percentage of monocytes in the *Wls* mutant bone marrow compared to the controls (Fig. 3I–K). In addition, the frequency of granulocytes was also slightly elevated, indicating the inflammation occurred at the bone marrow. IHC analysis with anti-CD4 antibody in the sections from P7 bone marrow validated the enrichment of T cells in the spongiosa area of primary ossification domain (Fig. 3L). These observations suggest that osteoblastic *Wls* prevents T cells and monocyte infiltration in the bone marrow under normal condition.

### Depletion of *Wls* in *Nestin*<sup>+</sup> mesenchymal progenitor cells impairs lymphopoiesis

*Nestin*-positive mesenchymal progenitor cells have recently been reported to serve as niches for HSCs and participate in osteogenic differentiation [41–43]. To obtain more extensive blockage of Wnt signaling in osteoblastic niches, we also generated the *Nestin-Cre; Wls*<sup>c/c</sup> mice that had *Wls* deletion at mesenchymal progenitor and osteoblast precursors stage. The mutant mice had a lifespan up to 18 days. The *Nestin-Cre; Wls*<sup>c/c</sup> mice were smaller in size and had

arrested growth from P7 as compared to the controls (Fig. 4A and D). The mutant mice also had a smaller spleen and thymus (Fig. 4A and B) and decreased bone ossification (Fig. 4E) as evidenced by HE staining. The *Wls* gene expression was decreased in the mutant mesenchymal stem cells isolated from plating (Fig. 4C). FACS analyses indicated that the frequencies of HSCs (Lin<sup>-</sup>Scal<sup>+</sup>c-Kit<sup>+</sup>CD127<sup>-</sup>, Fig. 4F, H, and I) and CLPs (Fig. 4G, J, and K) were not altered in the P12 BM of *Nestin-Cre; Wls*<sup>c/c</sup> mice. Similar to the osteoblastic *Wls* mutant mice, the impairment in B-cell lymphopoiesis was also observed in the bone marrow of *Nestin-Cre; Wls*<sup>c/c</sup> mice, which carried fewer frequencies of pro-B, pre-B, and immature B cells (Fig. 4L and M). The number but not the frequency of varied B-cell subpopulations was decreased in the spleens of mutant mice (Supporting Information Fig. 2A, B). Together with previous evidence, these observations indicate that Wnt proteins presented by mesenchymal progenitor cells sustain B-cell lymphopoiesis.

In addition, the CD4<sup>+</sup> and CD8<sup>+</sup> T-cell infiltration in the mutant bone marrow was quite evident (Fig. 5A, C, and D). Of note, similar to that in the *Col1-Cre; Wls*<sup>c/c</sup> mice, the majority of enriched T cells in the bone marrow and spleen of *Nestin-Cre; Wls*<sup>c/c</sup> mice were still CD62L<sup>+</sup>CD44<sup>-</sup> naive T cells (Fig. 5B and Supporting

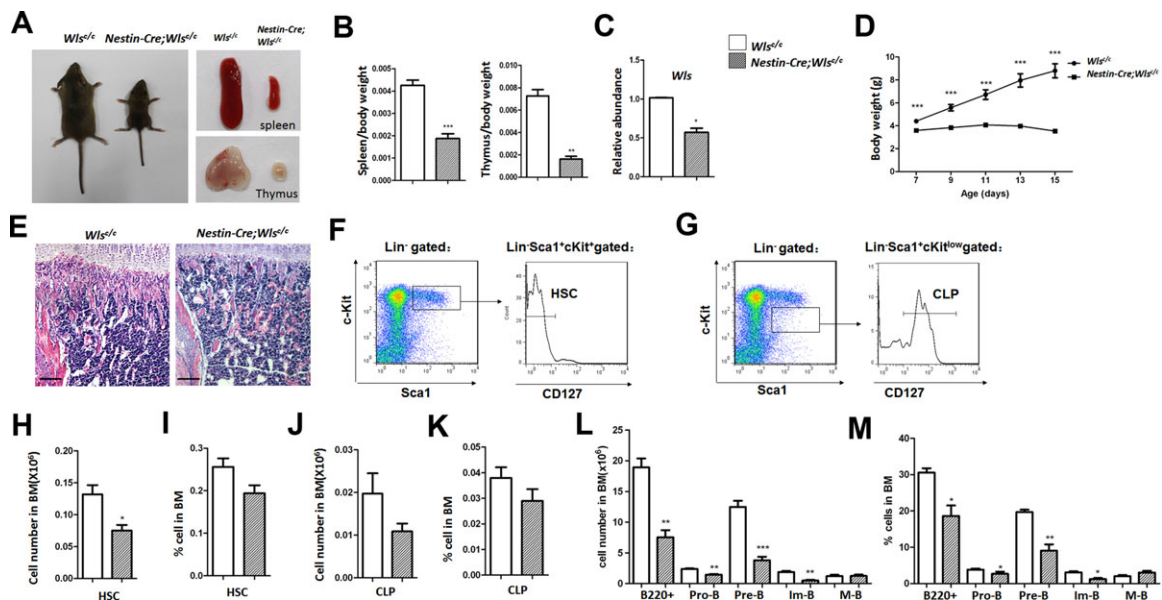


**Figure 4.** Defective B-cell lymphopoiesis in the *Nestin-Cre; Wls<sup>c/c</sup>* mice. (A) The sizes of the body (left panel), spleen, and thymus (right panel) size in the *Nestin-Cre; Wls<sup>c/c</sup>* mice. One representative picture out of six mice is shown. (B) The size of spleen and thymus relative to whole body. Bars show means  $\pm$  SEM from  $n = 6$  mice. White bar: *Wls<sup>c/c</sup>*, slash bar: *Nestin-Cre; Wls<sup>c/c</sup>*. (C) qRT-PCR showed the *Wls* expression in the bone marrow MSCs. Bars show means  $\pm$  SEM from  $n = 7$  mice of three independent experiments. (D) Growth curve of the *Nestin-Cre; Wls<sup>c/c</sup>* mice. Bars show means  $\pm$  SEM from  $n = 6$  mice. (E) HE staining of the trabecular bone of the distal femur. Bar, 50  $\mu$ m. One representative picture out of three mice is shown. (F, G) Dot plot depicts depict the HSC ( $\text{Lin}^- \text{Sca1}^+ \text{c-Kit}^+ \text{CD127}^-$ ) and CLP ( $\text{Lin}^- \text{Sca1}^+ \text{c-Kit}^- \text{CD127}^+$ ) populations. One representative dot plot out of five independent experiments is shown. (H, I) The cellularity and frequency of HSCs in the BM. Bars show means  $\pm$  SEM from  $n = 5$  mice. (J, K) The cellularity and frequency of CLPs in the BM ( $n = 6$ ). \* $p < 0.05$ . Bars show means  $\pm$  SEM from  $n = 5$  mice. (L, M) The frequencies and cellularity of pro-B cells, pre-B cells, and immature B-cells in the BM. Bars show means  $\pm$  SEM from  $n = 6$  mice. All the samples were collected at P12–P14 for both the controls and mutant mice. \* $p < 0.05$ , determined by Student's *t* test. BM, bone marrow.

Information Fig. 4E). In addition, the central memory T cells ( $\text{Tcm}$ ,  $\text{CD62L}^+ \text{CD44}^+$ ), but not effector memory T cells ( $\text{Tem}$ ,  $\text{CD62L}^- \text{CD44}^+$ ) were also enriched in the bone marrow of *Nestin-Cre; Wls<sup>c/c</sup>* mice (Fig. 5E and F). In contrast, they were not changed in the bone marrow of *Col1-Cre; Wls<sup>c/c</sup>* mice (Supporting Information Fig. 1C, D). Furthermore, the frequency of monocytes was relatively increased in the spleen (Supporting Information Fig. 2E, F), but not in the bone marrow (Supporting Information Fig. 2C, D). These observations indicate that no severe inflammation reaction is induced in the bone marrow of *Nestin-Cre; Wls<sup>c/c</sup>* mice. Deletion of *Wls* in *Nestin*<sup>+</sup> mesenchymal progenitor leads to naïve T-cell infiltration in the bone marrow.

### Deficiency of osteoblastic *Wls* does not affect HSCs maintenance and repopulation

Given that osteoblasts are pivotal niche cells for HSCs maintenance and self-renewal, we investigated the size and frequency of the HSCs pool in osteoblast-specific *Wls*-deficient mice. We first examined the LSKs, common lymphoid progenitors (CLPs) and multipotential progenitors (MPPs) in the bone marrow of *Col1-Cre; Wls<sup>c/c</sup>* mice, which were defined as  $\text{Lin}^- \text{Sca1}^+ \text{cKit}^+$ ,  $\text{Lin}^- \text{Sca1}^+ \text{cKit}^{\text{low}} \text{CD127}^+$ , and  $\text{Lin}^- \text{Sca1}^- \text{cKit}^+ \text{CD127}^-$ , respectively (Supporting Information Fig. 3A). The frequency and number of these progenitor populations were not altered in the P7 bone

marrow of *Col1-Cre; Wls<sup>c/c</sup>* mice compared to the controls (Supporting Information Fig. 3B–G). HSCs function is regulated by the proximity and dose of Wnt signaling activity [19, 44]. Therefore, to gain more efficient deletion of *Wls* in osteoblasts, we obtained the *Wls<sup>c/c</sup>* allele by crossing *Wls<sup>c/c</sup>* with *Actin-Cre* transgene. Then we generated the *Col1-Cre; Wls<sup>c/c</sup>* mice by crossing *Wls<sup>c/c</sup>* and *Col1-Cre; Wls<sup>c/c</sup>* mice. qRT-PCR confirmed that the depletion of *Wls* mRNA was nearly 80% in the osteoblasts obtained from the calvaria of *Col1-Cre; Wls<sup>c/c</sup>* mice (Fig. 6A).

Generally, HSCs are usually categorized into subpopulations of LT-HSCs, ST-HSCs, and MPPs (Fig. 6B). Lymphoid progenitor cells could be defined as CLPs whereas myeloid progenitor cells include CMPs, MEPs, and GMPs (Fig. 6E). In the bone marrow of *Col1-Cre; Wls<sup>c/c</sup>* mice, the frequencies and cell number of LT-HSCs, ST-HSCs, CLPs, CMPs, MEPs, and GMPs were normal relative to controls at P7 (Fig. 6C, D, F, G, H, and I). Only the percentage of LSKs ( $\text{Lin}^- \text{cKit}^+ \text{Sca1}^+$ ) and MPPs was slightly increased in the *Col1-Cre; Wls<sup>c/c</sup>* mutant (Fig. 6C). These data indicate that deficiency of osteoblastic *Wls* has a marked impact on HSCs frequency.

Then we conducted noncompetitive and competitive bone marrow transplantation (BMT) for the *Col1-Cre; Wls<sup>c/c</sup>* mice. Lethally irradiated wild-type B6.SJL recipient mice (CD45.1, 6-week old) were transplanted with  $6 \times 10^6$  BM-MNCs from wild-type or *Wls* mutant mice (CD45.2, one-week old). In the bone marrow at eight weeks after noncompetitive BMT assay, the frequencies

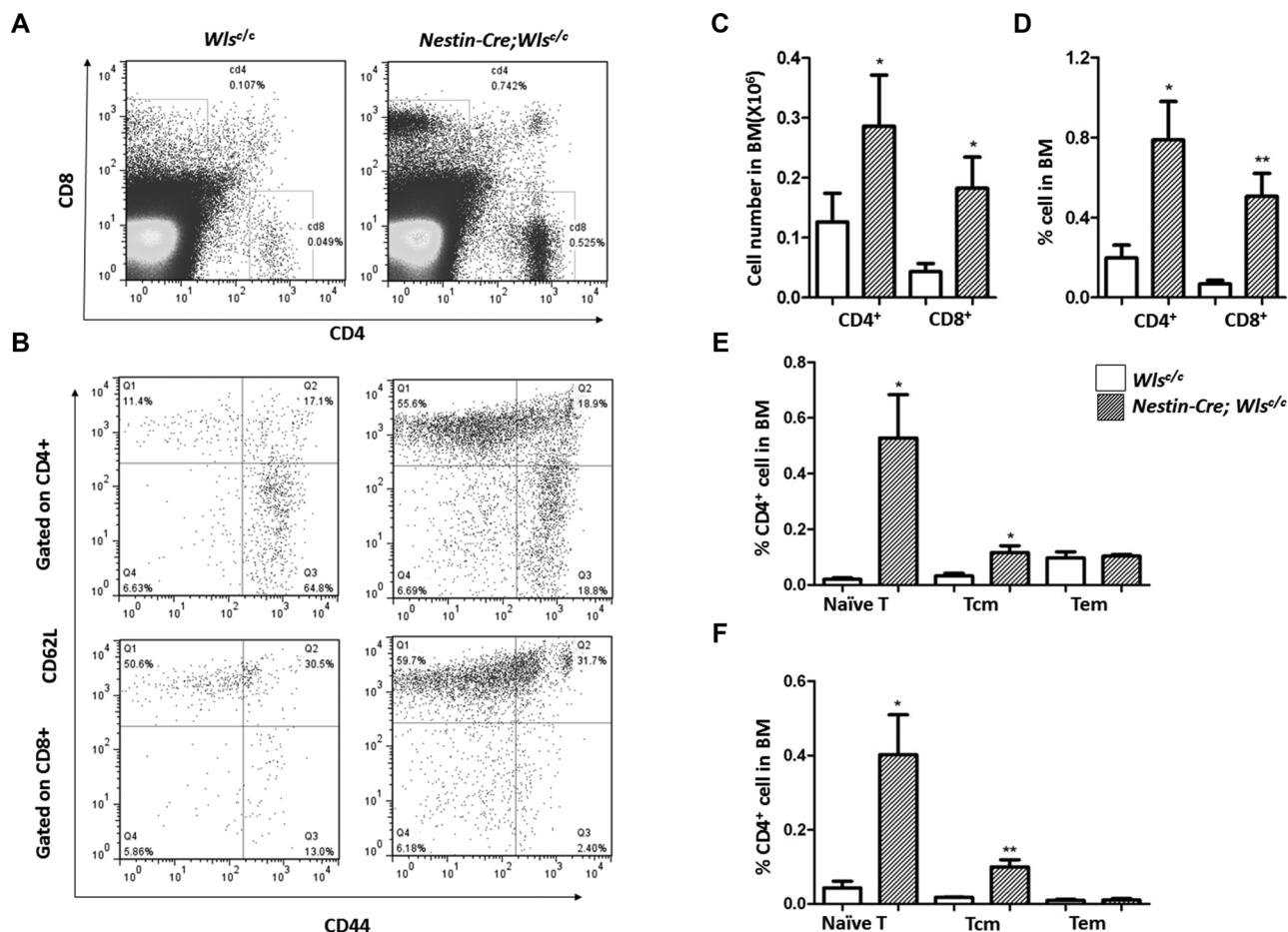


**Figure 5.** T-cell infiltration in the bone marrow of *Nestin-Cre; Wls<sup>c/c</sup>* mice. (A, B) Dot plots depict the T-cell subpopulations defined by CD4, CD8, CD62L, and CD44. One representative dot plot out of six independent experiments is shown. (C, D) The frequencies and cellularity of CD4<sup>+</sup> and CD8<sup>+</sup> cells in the BM. Bars show means  $\pm$  SEM from  $n = 6$  mice. White bar: *Wls<sup>c/c</sup>*, slash bar: *Nestin-Cre; Wls<sup>c/c</sup>*. (E, F) The frequencies of naïve T cells and central memory T cells (Tcm) in the BM. Bars show means  $\pm$  SEM from  $n = 6$  mice. All the samples were collected at P12–P14. \* $p < 0.05$ , determined by Student's *t* test. BM, bone marrow.

of CD45.2<sup>+</sup> HSCs and hematopoietic cells in BM were comparable between the *Wls* mutant and controls (data not shown). We then conducted a secondary non-competitive BMT based on the first BMT bone marrow reconstituted by the *Wls* mutant. Three months postsecondary noncompetitive BMT, the frequencies of CD45.2<sup>+</sup> LSKs, LT-HSCs, ST-HSCs, MPPs, and terminal hematopoietic cells were still comparable between the *Col1-Cre; Wls<sup>c/c</sup>* and control mice (Fig. 7A and B). In agreement, the frequencies of CD45.2<sup>+</sup> LSKs, LT-HSCs, ST-HSCs, MPPs, and terminal hematopoietic cells in the *Wls* mutant bone marrow were also indistinguishable from the controls after four months post competitive BMT (Fig. 7C and D). The *Wls* mutant mice displayed a slightly smaller pool of B220<sup>+</sup> B cells in peripheral blood from after four to 12 weeks postcompetitive BMT (Fig. 7E). Yet the B-cell populations recovered to normal from 12 weeks. In contrast, the frequencies of CD3e<sup>+</sup> T cells were comparable to the controls in the peripheral blood after four weeks postcompetitive BMT (Fig. 7F). Collectively, these findings suggest that deletion of *Wls* in osteoblasts exerts little effect on HSC maintenance and repopulation.

## Discussion

Osteoblasts and perivascular stromal cells facilitate B-cell differentiation. In our study, we investigated the overt role of Wnts in osteoblastic niches in supporting lymphopoiesis through ablation of *Wls* in osteoblast or perivascular mesenchymal progenitor cells. The *Wls*-deficient mice displayed defective B-cell development, indicating that osteoblastic Wnts act to sustain B-cell lymphopoiesis. In addition, defective B-cell differentiation in the mutant mice seems to be environment-dependent because B-cell lymphopoiesis progressively returned to normal after transplanting into a wild-type bone marrow microenvironment. These results highlight the complexity of the signaling cross-talk involved in bone marrow niches, which differ from the *in vitro* cultures of stromal cells.

B-cell development is regulated by several essential chemokines or cytokines, such as *IL-7* [24]. The expression of *IL-7* was decreased with loss of osteoblastic *Wls*, maybe resulting from a secondary effect with loss of Wnt signaling. A previous study has

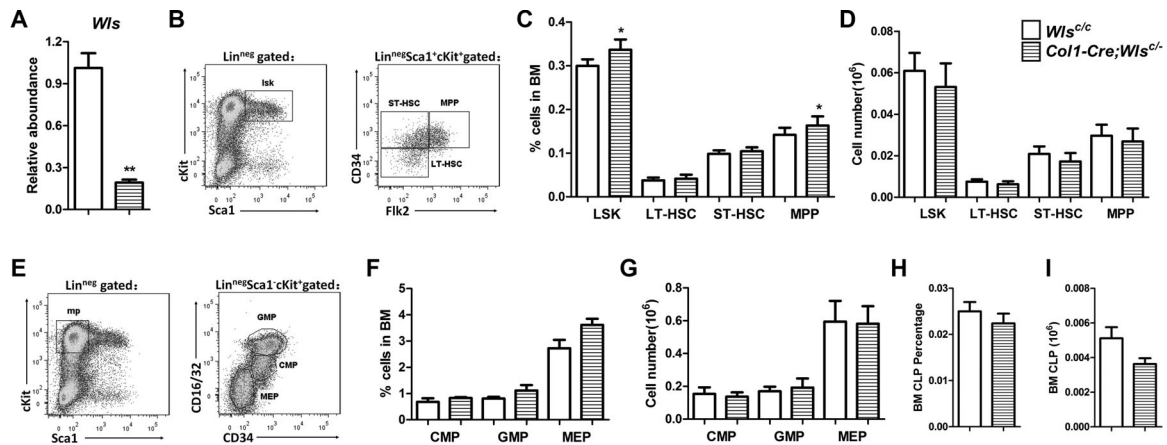


**Figure 6.** Deficiency of *Wls* in osteoblasts has marginal effect on HSCs pool. (A) qRT-PCR showed the *Wls* expression in the osteoblasts from calvaria of WT and *Col1-Cre; Wls<sup>c/c</sup>* mice. Bars show means  $\pm$  SEM from  $n = 3$  mice out of three independent experiments. White bar: *Wls<sup>c/c</sup>*, transverse bar: *Col1-Cre; Wls<sup>c/c</sup>*. (B) Dot plots depict the LT-HSCs ( $\text{Lin}^{-}\text{c-Kit}^{+}\text{Sca1}^{+}\text{CD34}^{-}\text{Flk2}^{-}$ ), ST-HSCs ( $\text{Lin}^{-}\text{c-Kit}^{+}\text{Sca1}^{+}\text{CD34}^{+}\text{Flk2}^{-}$ ), and MPPs ( $\text{Lin}^{-}\text{c-Kit}^{+}\text{Sca1}^{+}\text{CD34}^{+}\text{Flk2}^{+}$ ) populations. One representative dot plot out of four independent experiments is shown. (C, D) Histograms show the percentage (B) and cell number (C) of LSKs, LT-HSCs, ST-HSCs, and MPPs. Bars show means  $\pm$  SEM from  $n = 4$  mice. (E) Dot plots depict the myeloid cells including GMPs ( $\text{Lin}^{-}\text{c-Kit}^{+}\text{Sca1}^{-}\text{CD16/32}^{\text{high}}\text{CD34}^{\text{high}}$ ), MEPs ( $\text{Lin}^{-}\text{c-Kit}^{+}\text{Sca1}^{-}\text{CD16/32}^{\text{low}}\text{CD34}^{\text{low}}$ ), and CMPs ( $\text{Lin}^{-}\text{c-Kit}^{+}\text{Sca1}^{-}\text{CD16/32}^{\text{med}}\text{CD34}^{\text{med}}$ ). One representative dot plot out of four independent experiments is shown. (F, G) Histograms show the percentage (H) and cell number (I) of CMPs, GMPs, and MEPs. Bars show means  $\pm$  SEM from  $n = 4$  mice. (H, I) Histograms show the percentage (H) and absolute numbers (I) of CLPs. Bars show means  $\pm$  SEM from  $n = 7$  mice. All the samples were collected at P7. BM, bone marrow. \* $p < 0.05$ , determined by Student's *t* test.

reported that the *Sost*-deficient mice have a significant increase of canonical Wnt signaling activity, bone mass, and defective B-cell survival [23]. Therefore, the effect of osteoblastic Wnts on B-cell lymphopoiesis also involves the action of cytokines or chemokines that were induced by Wnt signaling in osteoblasts.

Another surprising outcome in the osteoblast-specific *Wls* knockout mice is an abnormal T-cell infiltration in the bone marrow. In response to antigen-induced inflammation, thymic naïve T cells migrate from thymus to targeted tissues and are activated to become effector and memory T cells. Of note, the  $\text{CD8}^{+}$  memory T cells seed in bone marrow as adult stem cells after inflammation [45, 46]. In our study, naïve T cells and central memory T cells were attracted to the bone marrow of *Nestin-Cre; Wls<sup>c/c</sup>* mice.  $\text{CD4}^{+}$  and  $\text{CD8}^{+}$  T cells were enriched in the bone marrow of *Col1-Cre; Wls<sup>c/c</sup>* mice, coupled with the decrease of *Wnt5a* protein level in the mutant bone marrow. *Wnt5a* has been reported to be required for the *Cxcl12*-mediated T-cell migration and infiltration [47]. These findings indicate osteoblastic Wnts may have indirect roles in memory T-cell seeding in bone marrow.

Osteoblasts have been reported to be important niche cells for HSC activity. The responses of HSCs in maintenance and differentiation are determined by their proximity, doses, cross-talk, and competition with multiple Wnt ligands in niches [44]. Unexpectedly, *Wls* deficiency in the osteoblasts had no obvious impact on HSCs maintenance and repopulation based on BMT assays. These results may arise from the insufficient deletion of *Wls* or compensated action of various Wnt proteins that are abundant in the bone marrow. Given the overt defective B-cell lymphopoiesis and marginal impact on the HSCs pool with loss of osteoblastic *Wls*, the osteoblasts may primarily confer niches for lymphoid progenitor cells instead of HSCs, which are also suggested by previous reports

[7, 9]. In summary, we observed a supportive effect of osteoblastic Wnts on B-cell development, a protective role for T-cell infiltration and a marginal influence on the HSCs pool. These findings provide new insights into the role of Wnt signaling in regulating B-cell lymphopoiesis and HSCs maintenance, and also present clues for the mechanism of T-cell infiltration in bone marrow.

## Materials and methods

### Mice

Conditional knockout mice were generated by crossing the *Wls<sup>c/c</sup>* with *Col1-Cre* (3.6 kb promoter) or *Nestin-Cre* transgenic mice [48, 49]. Mice carrying the *Wls<sup>c/c</sup>* floxed allele [39] were crossed with *Actin-Cre* (Jackson Laboratories) transgenic mice to obtain the *Wls* null allele (*Actin-Cre; Wls<sup>+/-</sup>*). The *Wls<sup>+/-</sup>* mice were crossed with *Wls<sup>c/c</sup>* to obtain *Wls<sup>c/-</sup>* mice. Then the *Wls<sup>c/c</sup>* or *Wls<sup>c/-</sup>* mice were crossed with the *Col1-Cre* mice to obtain *Col1-Cre; Wls<sup>c/c</sup>* or *Col1-Cre; Wls<sup>c/-</sup>* mice. Mice were maintained in a specific pathogen-free environment with free access to food and water and a 12/12 light–dark cycle. All animal experiments were conducted in accordance with guidelines set by Bio-X Institutes in Shanghai Jiao Tong University.

### Histological analysis

The bones from mice collected at the indicated time were first fixed in 4% PFA at 4°C overnight, then decalcified in 15% EDTA for

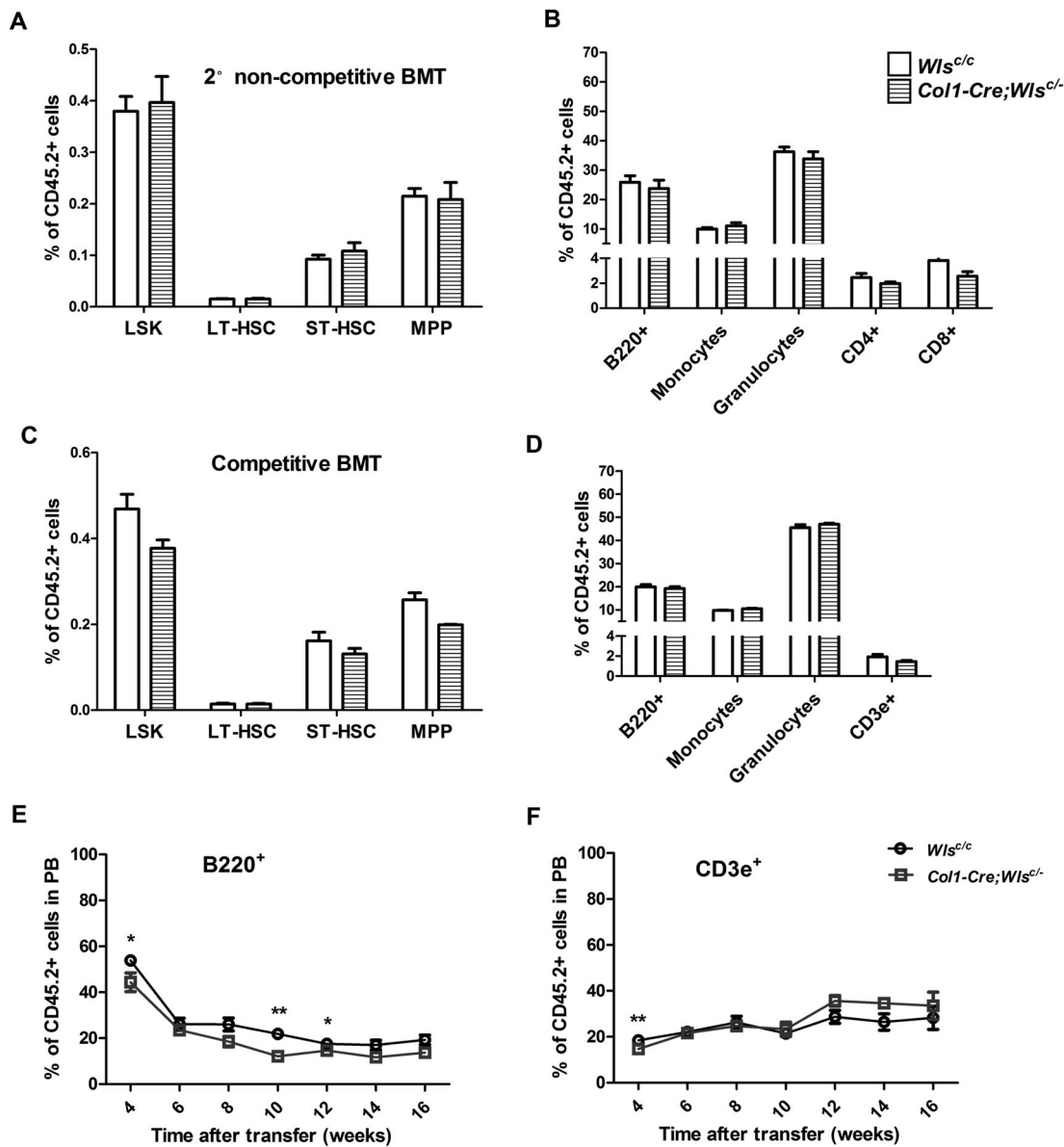


**Figure 7.** Loss of *Wls* in osteoblasts has no influence on HSC repopulation. (A, B) The frequencies of CD45.2<sup>+</sup> LSKs, LT-HSCs, ST-HSCs, MPPs (A) and terminal differentiated hematopoietic cells (B) were comparable in the BM of wild type (*n* = 7) and *Col1-Cre; Wls<sup>c/-</sup>* (*n* = 8) mice in the secondary noncompetitive BMT assay. The second BMT was conducted at eight weeks after the first BMT. Hematopoiesis was analyzed for HSCs after three months of secondary BMT. Bars show means ± SEM from recipient mice with pooled BM transplantation. White bar: *Wls<sup>c/c</sup>*, transverse bar: *Col1-Cre; Wls<sup>c/-</sup>*. (C, D) The frequencies of CD45.2<sup>+</sup> LSKs, LT-HSCs, ST-HSCs, MPPs (C) and terminal differentiated hematopoietic cells (D) in the BM after four months of competitive BMT. Bars show means ± SEM from *n* = 7 mice. (E, F) The frequency of the B220<sup>+</sup> and CD3e<sup>+</sup> in CD45.2<sup>+</sup> cells in the PB of recipients during four months after competitive BMT. Bars show means ± SEM from *n* = 7 mice. BM, bone marrow; PB, peripheral blood; BMT, bone marrow transplantation. \**p* < 0.05, determined by Student's *t* test.

several days, and finally embedded in paraffin. Paraffin embedding and HE staining was conducted as standard procedures. Longitudinal sections (10 μm) were cut through the trabecular region.

### Cell preparation and FACS

After the mice were killed with standard procedures, the spleen and thymus were weighed with balance relative to the whole body. For FACS cell preparations, whole bone marrow were flushed out

with PBS supplemented with 2% FBS (Gibco). Spleen and thymus were dissected into small pieces by forceps and gently squashed by syringe, then were suspended with PBS plus 2% FBS. Spleen cells and peripheral blood cells required an additional procedure for red blood cell lysis. Cells were filtered through a 70 μm cell strainer. The cell number of each organ was quantified as cellularity. Cell suspensions were first treated with Fc Block (BD Pharmingen) and then incubated with antibody combinations. The following antibodies were obtained from eBioscience: biotin-labeled lineage markers B220, CD11b, CD11c, Gr-1, Ter-119,

NK-1.1, CD3, CD4, CD8a, TCR $\beta$ , TCR $\gamma\delta$ , CD127; PerCP-Cy5.5, PE, FITC, allophycocyanin, and allophycocyanin-Cy7-conjugated streptavidin; and Sca-1-FITC, c-Kit- allophycocyanin, CD135-PerCP-eFluor710, CD62L-PE, CD34-PE, B220-PerCP-Cy5.5, IgD-FITC, CD19- allophycocyanin, CD11b-Alexa Fluor 488, Gr-1-PE, CD4- allophycocyanin, CD8a-PerCP-Cy5.5, CD45.1-eFluor 605NC, and CD45.2-eFluor 450. CD43-allophycocyanin, IgM-PE, AA4.1-PE were obtained from BD Pharmingen. Cells were analyzed on a FACS Fortessa or FACS Calibur instrument, and data were analyzed using FlowJo software.

### Bone marrow transplantation

Recipient mice were irradiated using an X-ray source (RAD Source) delivering approximately 1.01 Gy/min. After receiving two doses of 4.75 Gy at a 4-h interval, recipient mice were transplanted with  $6 \times 10^6$  donor cells and then treated with antibiotics (100 mg/L neomycin sulfate and 10 mg/L polymyxin B sulfate) for two weeks after transplantation. For competitive transplantation,  $3 \times 10^6$  wild type or *Col1-Cre; Wls<sup>+/−</sup>* (CD45.2) BM cells were mixed with  $3 \times 10^6$  cells from the wild type (CD45.1) before they were transplanted into wild-type recipient mice (CD45.1). Cells were injected into recipient mice through tail vein injection. The hematopoiesis in the peripheral blood was monitored for 16 weeks after BMT. For the noncompetitive BMT assay,  $6 \times 10^6$  *Col1-Cre; Wls<sup>+/−</sup>* (CD45.2) BM cells were directly transplanted into wild-type recipient mice (CD45.1). After two months, the recipient bone marrow underwent secondary BMT following the procedures in the first BMT. Three months after the secondary BMT, hematopoiesis in the bone marrow was analyzed by FACS.

### qRT-PCR

To isolate RNA from osteoblasts of cortical bone for qRT-PCR, cortical bones from the mutant mice were removed soft tissues (including skin, muscle et al.), and flushed out the bone marrow with PBS for several times. Then the diaphyses of cortical bones were cut into small pieces of approx 1–2 mm<sup>2</sup> with scissors and grinded into power in liquid nitrogen. To isolate RNA from calvarial osteoblasts in the *Col1-Cre; Wls<sup>+/−</sup>* mice at P7 for qRT-PCR, euthanize the mice, clean the head using 70% ethanol, remove the skin from the top of the head, wash the calvariae with PBS and remove the soft tissues, chop the bones into small fragments of approx 1–2 mm<sup>2</sup>. Then osteoblasts were also collected from the calvaria bones by five times of 15-min digestion with Collagenase II (2.5 mg/mL) and Trypsin (0.05%). Cells from the last two or three digestions are combined. RNA was extracted from bone cells using Trizol reagent (Invitrogen) according to standard procedures. SuperScript III Reverse Transcriptase (Invitrogen) was used to synthesize cDNA. Real-time PCR was performed with an ABI Prism 7500 Sequence Detection System (Applied Biosystems) using a SYBR Green Kit (Roche). The samples were normalized to  $\beta$ -actin expression. Oligos for

qRT-PCR: *Wntless* –F, 5'-ACCGTGATGATATGTTTTCTG-3', *Wntless*-R, 5'-TACCACACCATAATGATGA A-3'; *IL-7*–F, 5'-TCCTCCAC TGATCCTTGTCT-3', *IL-7*–R, 5'-GGTTCATTATTCGGGCAAT-3'.

### ELISA assay

The mice were euthanized to obtain long bones. The bone marrow was flushed out with 1.5 mL PBS per mouse, then the supernatant was collected for ELISA assay by centrifuging the cell suspension for 5 min at  $300 \times g$ .

### Statistics

Statistical analysis was performed by Student's *t* test using GraphPad Prism 5 software. Data are represented as means  $\pm$  SEM and significance was set at  $p \leq 0.05$ .

**Acknowledgments:** This work was supported by research funding from the National Major Fundamental Research 973 Program of China [2014CB942902 and 2012CB966903] and grants from the National Natural Science Foundation of China [31171396, 31271553, 81421061, 31100624 and 81200586].

**Conflict of interest:** The authors declare no commercial or financial conflict of interest.

### References

- Wilson, A. and Trumpp, A., Bone-marrow haematopoietic-stem-cell niches. *Nat. Rev. Immunol.* 2006. 6: 93–106.
- Sugiyama, T., Kohara, H., Noda, M. and Nagasawa, T., Maintenance of the hematopoietic stem cell pool by CXCL12-CXCR4 chemokine signaling in bone marrow stromal cell niches. *Immunity* 2006. 25: 977–988.
- Ding, L., Saunders, T. L., Enikolopov, G. and Morrison, S. J., Endothelial and perivascular cells maintain haematopoietic stem cells. *Nature* 2012. 481: 457–462.
- Hooper, A. T., Butler, J. M., Nolan, D. J., Kranz, A., Iida, K., Kobayashi, M., Kopp, H. G. et al., Engraftment and reconstitution of hematopoiesis is dependent on VEGFR2-mediated regeneration of sinusoidal endothelial cells. *Cell Stem Cell* 2009. 4: 263–274.
- Zhang, J., Niu, C., Ye, L., Huang, H., He, X., Tong, W. G., Ross, J. et al., Identification of the haematopoietic stem cell niche and control of the niche size. *Nature* 2003. 425: 836–841.
- Calvi, L. M., Adams, G. B., Weibrecht, K. W., Weber, J. M., Olson, D. P., Knight, M. C., Martin, R. P. et al., Osteoblastic cells regulate the haematopoietic stem cell niche. *Nature* 2003. 425: 841–846.
- Greenbaum, A., Hsu, Y. M., Day, R. B., Schuettpelz, L. G., Christopher, M. J., Borgerding, J. N., Nagasawa, T. et al., CXCL12 in early

- mesenchymal progenitors is required for haematopoietic stem-cell maintenance. *Nature* 2013. **495**: 227–230.
- 8 Sacchetti, B., Funari, A., Michienzi, S., Di Cesare, S., Piersanti, S., Saggio, I., Tagliafico, E. et al., Self-renewing osteoprogenitors in bone marrow sinusoids can organize a hematopoietic microenvironment. *Cell* 2007. **131**: 324–336.
  - 9 Ding, L. and Morrison, S. J., Haematopoietic stem cells and early lymphoid progenitors occupy distinct bone marrow niches. *Nature* 2013. **495**: 231–235.
  - 10 Morrison, S. J. and Scadden, D. T., The bone marrow niche for haematopoietic stem cells. *Nature* 2014. **505**: 327–334.
  - 11 Kikuchi, A., Yamamoto, H., Sato, A. and Matsumoto, S., New insights into the mechanism of Wnt signaling pathway activation. *Int. Rev. Cell Mol. Biol.* 2011. **291**: 21–71.
  - 12 Kirstetter, P., Anderson, K., Porse, B. T., Jacobsen, S. E. and Nerlov, C., Activation of the canonical Wnt pathway leads to loss of hematopoietic stem cell repopulation and multilineage differentiation block. *Nat. Immunol.* 2006. **7**: 1048–1056.
  - 13 Reya, T., Duncan, A. W., Ailles, L., Domen, J., Scherer, D. C., Willert, K., Hintz, L. et al., A role for Wnt signalling in self-renewal of haematopoietic stem cells. *Nature* 2003. **423**: 409–414.
  - 14 Luis, T. C., Weerkamp, F., Naber, B. A., Baert, M. R., deHaas, E. F., Nikolic, T., Heuvelmans, S. et al., Wnt3a deficiency irreversibly impairs hematopoietic stem cell self-renewal and leads to defects in progenitor cell differentiation. *Blood* 2009. **113**: 546–554.
  - 15 Zhao, C., Blum, J., Chen, A., Kwon, H. Y., Jung, S. H., Cook, J. M., Lagoo, A. et al., Loss of beta-catenin impairs the renewal of normal and CML stem cells in vivo. *Cancer Cell* 2007. **12**: 528–541.
  - 16 Koch, U., Wilson, A., Cobas, M., Kemler, R., Macdonald, H. R. and Radtke, F., Simultaneous loss of beta- and gamma-catenin does not perturb hematopoiesis or lymphopoiesis. *Blood* 2008. **111**: 160–164.
  - 17 Cobas, M., Wilson, A., Ernst, B., Mancini, S. J., MacDonald, H. R., Kemler, R. and Radtke, F., Beta-catenin is dispensable for hematopoiesis and lymphopoiesis. *J. Exp. Med.* 2004. **199**: 221–229.
  - 18 Fleming, H. E., Janzen, V., Lo Celso, C., Guo, J., Leahy, K. M., Kronenberg, H. M. and Scadden, D. T., Wnt signaling in the niche enforces hematopoietic stem cell quiescence and is necessary to preserve self-renewal in vivo. *Cell Stem Cell* 2008. **2**: 274–283.
  - 19 Luis, T. C., Naber, B. A., Roozen, P. P., Brugman, M. H., de Haas, E. F., Ghazvini, M., Fibbe, W. E. et al., Canonical Wnt signaling regulates hematopoiesis in a dosage-dependent fashion. *Cell Stem Cell* 2011. **9**: 345–356.
  - 20 Florian, M. C., Nattamai, K. J., Dorr, K., Marka, G., Uberle, B., Vas, V., Eckl, C. et al., A canonical to non-canonical Wnt signalling switch in haematopoietic stem-cell ageing. *Nature* 2013. **503**: 392–396.
  - 21 Verovskaya, E. and de Haan, G., Noncanonical wnt comes of age in hematopoietic stem cells. *Cell Stem Cell* 2013. **13**: 642–643.
  - 22 Zhu, J., Garrett, R., Jung, Y., Zhang, Y., Kim, N., Wang, J., Joe, G. J. et al., Osteoblasts support B-lymphocyte commitment and differentiation from hematopoietic stem cells. *Blood* 2007. **109**: 3706–3712.
  - 23 Cain, C. J., Rueda, R., McLelland, B., Collette, N. M., Loots, G. G. and Manilay, J. O., Absence of sclerostin adversely affects B-cell survival. *J. Bone Miner. Res.* 2012. **27**: 1451–1461.
  - 24 Clark, M. R., Mandal, M., Ochiai, K. and Singh, H., Orchestrating B cell lymphopoiesis through interplay of IL-7 receptor and pre-B cell receptor signalling. *Nat. Rev. Immunol.* 2014. **14**: 69–80.
  - 25 Qian, Z., Chen, L., Fernald, A. A., Williams, B. O. and LeBeau, M. M., A critical role for Apc in hematopoietic stem and progenitor cell survival. *J. Exp. Med.* 2008. **205**: 2163–2175.
  - 26 Ranheim, E. A., Kwan, H. C., Reya, T., Wang, Y. K., Weissman, I. L. and Francke, U., Frizzled 9 knock-out mice have abnormal B-cell development. *Blood* 2005. **105**: 2487–2494.
  - 27 Reya, T., O’Riordan, M., Okamura, R., Devaney, E., Willert, K., Nusse, R. and Grosschedl, R., Wnt signaling regulates B lymphocyte proliferation through a LEF-1 dependent mechanism. *Immunity* 2000. **13**: 15–24.
  - 28 Yu, Q., Quinn, W. J., 3rd, Salay, T., Crowley, J. E., Cancro, M. P. and Sen, J. M., Role of beta-catenin in B cell development and function. *J. Immunol.* 2008. **181**: 3777–3783.
  - 29 Dosen, G., Tenstad, E., Nygren, M. K., Stubberud, H., Funderud, S. and Rian, E., Wnt expression and canonical Wnt signaling in human bone marrow B lymphopoiesis. *BMC Immunol.* 2006. **7**: 13.
  - 30 Malhotra, S., Baba, Y., Garrett, K. P., Staal, F. J., Gerstein, R. and Kincade, P. W., Contrasting responses of lymphoid progenitors to canonical and noncanonical Wnt signals. *J. Immunol.* 2008. **181**: 3955–3964.
  - 31 Ichii, M., Frank, M. B., Iozzo, R. V. and Kincade, P. W., The canonical Wnt pathway shapes niches supportive of hematopoietic stem/progenitor cells. *Blood* 2012. **119**: 1683–1692.
  - 32 Banziger, C., Soldini, D., Schutt, C., Zipperlen, P., Hausmann, G. and Basler, K., Wntless, a conserved membrane protein dedicated to the secretion of Wnt proteins from signaling cells. *Cell* 2006. **125**: 509–522.
  - 33 Adell, T., Salo, E., Boutros, M. and Bartscherer, K., Smed-Evi/Wntless is required for beta-catenin-dependent and -independent processes during planarian regeneration. *Development* 2009. **136**: 905–910.
  - 34 Kim, H., Cheong, S. M., Ryu, J., Jung, H. J., Jho, E. H. and Han, J. K., Xenopus Wntless and the retromer complex cooperate to regulate XWnt4 secretion. *Mol. Cell Biol.* 2009. **29**: 2118–2128.
  - 35 Fu, J., Ivy Yu, H. M., Maruyama, T., Mirando, A. J. and Hsu, W., Gpr177/mouse Wntless is essential for Wnt-mediated craniofacial and brain development. *Dev. Dyn.* 2011. **240**: 365–371.
  - 36 Zhu, X., Zhu, H., Zhang, L., Huang, S., Cao, J., Ma, G., Feng, G. et al., Wnt-mediated Wnts differentially regulate distal limb patterning and tissue morphogenesis. *Dev. Biol.* 2012. **365**: 328–338.
  - 37 Myung, P. S., Takeo, M., Ito, M. and Atit, R. P., Epithelial Wnt ligand secretion is required for adult hair follicle growth and regeneration. *J. Invest. Dermatol.* 2012. **133**: 31–41.
  - 38 Zhong, Z., Zylstra-Diegel, C. R., Schumacher, C. A., Baker, J. J., Carpenter, A. C., Rao, S., Yao, W. et al., Wntless functions in mature osteoblasts to regulate bone mass. *Proc. Natl. Acad. Sci. USA* 2012. **109**: E2197–E2204.
  - 39 Wan, Y., Lu, C., Cao, J., Zhou, R., Yao, Y., Yu, J., Zhang, L. et al., Osteoblastic Wnts differentially regulate bone remodeling and the maintenance of bone marrow mesenchymal stem cells. *Bone* 2013. **55**: 258–267.
  - 40 Kikuchi, K., Lai, A. Y., Hsu, C. L. and Kondo, M., IL-7 receptor signaling is necessary for stage transition in adult B cell development through up-regulation of EBF. *J. Exp. Med.* 2005. **201**: 1197–1203.
  - 41 Mendez-Ferrer, S., Michurina, T. V., Ferraro, F., Mazloom, A. R., MacArthur, B. D., Lira, S. A., Scadden, D. T. et al., Mesenchymal and haematopoietic stem cells form a unique bone marrow niche. *Nature* 2010. **466**: 829–834.
  - 42 Noriaki Ono, W. O., Toshihide Mizoguchi, Takashi Nagasawa, Paul S. Frenette and Henry M. Kronenberg, Vasculature-associated cells expressing nestin in developing bones encompass early cells in the osteoblast and endothelial lineage. *Dev. Cell* 2014. **29**: 10.
  - 43 Mizoguchi, T., Pinho, S., Ahmed, J., Kunisaki, Y., Hanoun, M., Mendelson, A., Ono, N. et al., Osterix marks distinct waves of primitive and definitive

- stromal progenitors during bone marrow development. *Dev. Cell* 2014. **29**: 10.
- 44 Zhang, J. and Li, L., Stem cell niche: microenvironment and beyond. *J. Biol. Chem.* 2008. **283**: 9499–9503.
- 45 Becker, T. C., Coley, S. M., Wherry, E. J. and Ahmed, R., Bone marrow is a preferred site for homeostatic proliferation of memory CD8 T cells. *J. Immunol.* 2005. **174**: 1269–1273.
- 46 Graef, P., Buchholz, V. R., Stemberger, C., Flossdorf, M., Henkel, L., Schiemann, M., Drexler, I. et al., Serial transfer of single-cell-derived immunocompetence reveals stemness of CD8(+) central memory T cells. *Immunity* 2014. **41**: 116–126.
- 47 Ghosh, M. C., Collins, G. D., Vandanmagsar, B., Patel, K., Brill, M., Carter, A., Lustig, A. et al., Activation of Wnt5A signaling is required for CXC chemokine ligand 12-mediated T-cell migration. *Blood* 2009. **114**: 1366–1373.
- 48 Zha, L., Hou, N., Wang, J., Yang, G., Gao, Y., Chen, L. and Yang, X., Collagen1alpha1 promoter drives the expression of Cre recombinase in osteoblasts of transgenic mice. *J. Genet. Genomics* 2008. **35**: 525–530.
- 49 Dubois, N. C., Hofmann, D., Kaloulis, K., Bishop, J. M. and Trumpp, A., Nestin-Cre transgenic mouse line Nes-Cre1 mediates highly efficient

Cre/loxP mediated recombination in the nervous system, kidney, and somite-derived tissues. *Genesis* 2006. **44**: 355–360.

**Abbreviations:** BM: bone marrow · CLP: common lymphoid progenitor · MPP: multipotential progenitor · Wls: Wntless

**Full correspondence:** Dr. Xizhi Guo Bio-X Institutes, Key Laboratory for the Genetics of Developmental and Neuropsychiatric Disorders (Ministry of Education), Shanghai Jiao Tong University, #800 Dongchuan Road, Biomedical Bldg#1-205, Shanghai 200240, China e-mail: xzguo2005@sjtu.edu.cn

**Additional correspondence:** Dr. Zhengju Yao, Bio-X Institutes, Key Laboratory for the Genetics of Developmental and Neuropsychiatric Disorders (Ministry of Education), Shanghai Jiao Tong University, Shanghai 200240, China e-mail: zjyao@sjtu.edu.cn

Received: 11/12/2014

Revised: 29/4/2015

Accepted: 7/7/2015

Accepted article online: 14/7/2015